# Development & Validation of Low-Cost, Highly-Durable, Spinel-Based Materials for SOFC Cathode-Side Contact

**Jiahong Zhu**

**Department of Mechanical Engineering**

**Tennessee Technological University (TTU)**

***20th Annual Solid Oxide Fuel Cell (SOFC) Project Review Meeting***

***Nov. 16-18, 2021***

# Outline

- Introduction and Project Objectives
- Effect of Spinel Composition on the Reaction Layer Formation
- Performance Evaluation of the Sintered Spinel Contact Thermally Converted from Metallic Precursors
- Reactive Sintering of Dense $(Mn,Co)_3O_4$ (MCO) Coatings
- Co-sintering of Spinel-Based Coating/Contact Dual-Layer Structure
- Concluding Remarks
- Acknowledgments

# Need of Contacting for Different SOFC Stacks

- In stacks with anode-supported cells (ASC-SOFC), the contact is required to minimize the cathode-interconnect interfacial resistance.

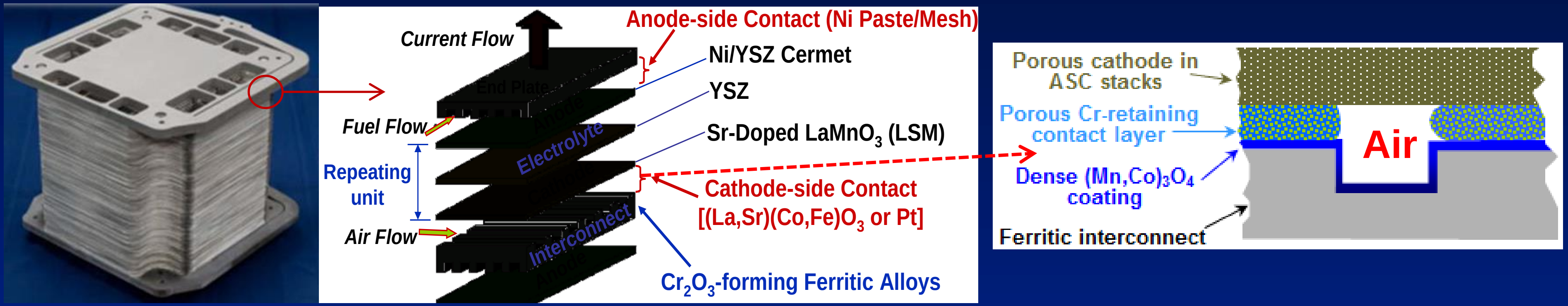


*Cathode-Interconnect Interface in ASC SOFC Stacks*

- In all-ceramic stacks, the contact is required to minimize the interfacial resistance between the current collector plate and cathode end plate.

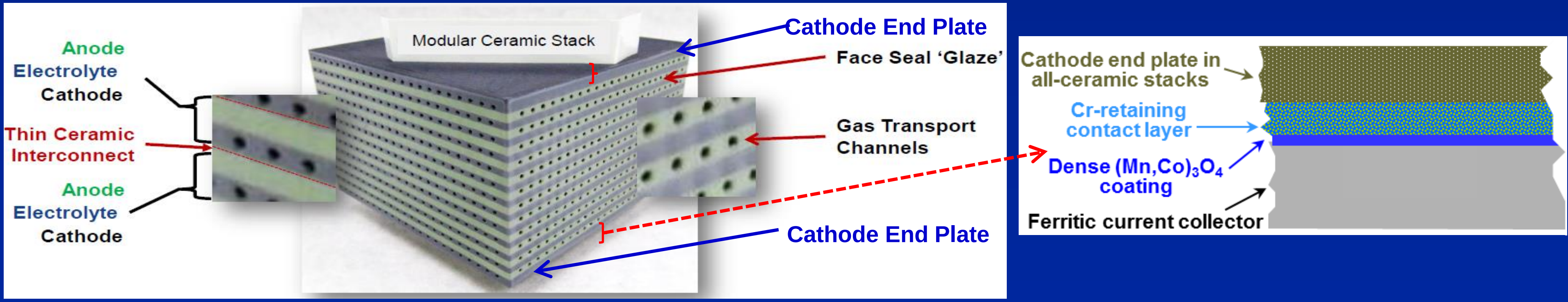


*Cathode-Current Collector Interface in All-Ceramic SOFC Stacks*

# Different Contact Materials

- Key contact material requirements are: low cost, high electrical conductivity, good CTE match, adequate compatibility and sinterability
- Most contact developments have focused on (La,Sr)(Mn,Co,Fe,Ni,Cu)$O_3$:
  - Difficulty in balancing the electrical conductivity, CTE, sinterability and chemical compatibility of the perovskites.

| Material Type | Example | CTE ($\times 10^{-6}$/K) (20–800°C) | Conductivity ($S \cdot cm^{-1}$, 800°C) | Main Concern |
|---|---|---|---|---|
| Noble Metal | Pt | 10.0 | Metallic | High Cost |
| | Pd | 12.3 | Metallic | High Cost |
| | Au | 16.6 | Metallic | High Cost |
| | Ag | 22.0 | Metallic | Volatility |
| Perovskite | $(La_{0.8}Sr_{0.2})\ CoO_{3-\delta}$ | 19.2 (20-1000°C) | 1400 | CTE Mismatch |
| | $(La_{0.8}Sr_{0.2})(Co_{0.5}Fe_{0.5})O_{3-\delta}$ | 18.3 (20-1000°C) | 340 | CTE Mismatch |
| | $(La_{0.8}Sr_{0.2})(Co_{0.5}Mn_{0.5})O_{3-\delta}$ | 15.0 (20-1000°C) | 190 | CTE Mismatch |
| | $(La_{0.8}Sr_{0.2})MnO_3$ | 11.7 (20-1000°C) | 170 | Sinterability |
| | $LaMn_{0.45}Co_{0.35}Cu_{0.2}O_3$ | 13.9 | 80 | Mn/Cu Migration |
| Spinel | $MnCo_2O_4$ | 9.7-14.4 | 24- 89 | Sinterability |
| | $Mn_{1.5}Co_{1.5}O_4$ | 10.6-11.6 | 55-68 | Sinterability |
| | $NiCo_2O_4$ | 12.1 | 0.93 | Sinterability |
| | $NiFe_2O_4$ | 11.8 | 0.3, 6.8, 17.1 | Sinterability |

# Why $(Ni,Fe)_3O_4$- and $(Mn,Co)_3O_4$-Based Spinels as Contact Material?

- **Conductive spinels based on $(Ni,Fe)_3O_4$ and $(Mn,Co)_3O_4$, which have been extensively evaluated as interconnect coating, are also promising for contact application, based on electrical conductivity, CTE, chemical compatibility, etc.**

| Material Type | Example | CTE ($\times10^{-6}$/K) (20–800°C) | Conductivity ($S\cdot cm^{-1}$, 800°C) | Main Concern |
|---|---|---|---|---|
| Spinel | $MnCo_2O_4$ | 9.7-14.4 | 24- 89 | Sinterability |
| | $Mn_{1.5}Co_{1.5}O_4$ | 10.6-11.6 | 55-68 | Sinterability |
| | $NiCo_2O_4$ | 12.1 | 0.93 | Sinterability |
| | $NiFe_2O_4$ | 11.8 | 0.3, 6.8, 17.1 | Sinterability |
| | $Ni_{0.85}Fe_{2.15}O_4$ | 12.1 | 15.4 | Sinterability |

- **Unfortunately, the sinterability of spinels is very poor (typically ≥1000°C), if metal oxides are used as the starting powders.**

- **Employment of metallic powders (instead of oxide powders) as the starting precursor will lower the sintering temperature via a reactive sintering mechanism called <u>e</u>nvironmentally-<u>a</u>ssisted <u>r</u>eactive <u>s</u>intering (EARS).**

# Utilization of EARS for Reduced-Temperature Sintering of Spinel-Based Contact

- **In EARS, with the participation of oxygen from air, the metallic powder precursor will be oxidized and reacted to form a well-sintered spinel at a reduced temperature (e.g., 900°C):**

$$\text{(b)}: AO_x + 2BO_y + (2-\tfrac{1}{2}x-y)O_2(g) = AB_2O_4 + \Delta H_1$$

$$\text{(c)}: A + 2BO_y + (2-y)O_2(g) = AB_2O_4 + \Delta H_2$$

$$\text{(d) \& (e)}: A + 2B + 2O_2(g) = AB_2O_4 + \Delta H_3$$

$$\Delta H_3 > \Delta H_2 \gg \Delta H_1$$

- **Enhanced sintering via EARS is likely due to:**
  - **Heat released during the reaction;**
  - **Volume expansion upon conversion of metal to metal oxide;**
  - **Formation of highly-active surface nano-oxides;**
  - **Shorter diffusion distance when a pre-alloyed powder is employed.**

*Zhu et al., IJHE, 2018*

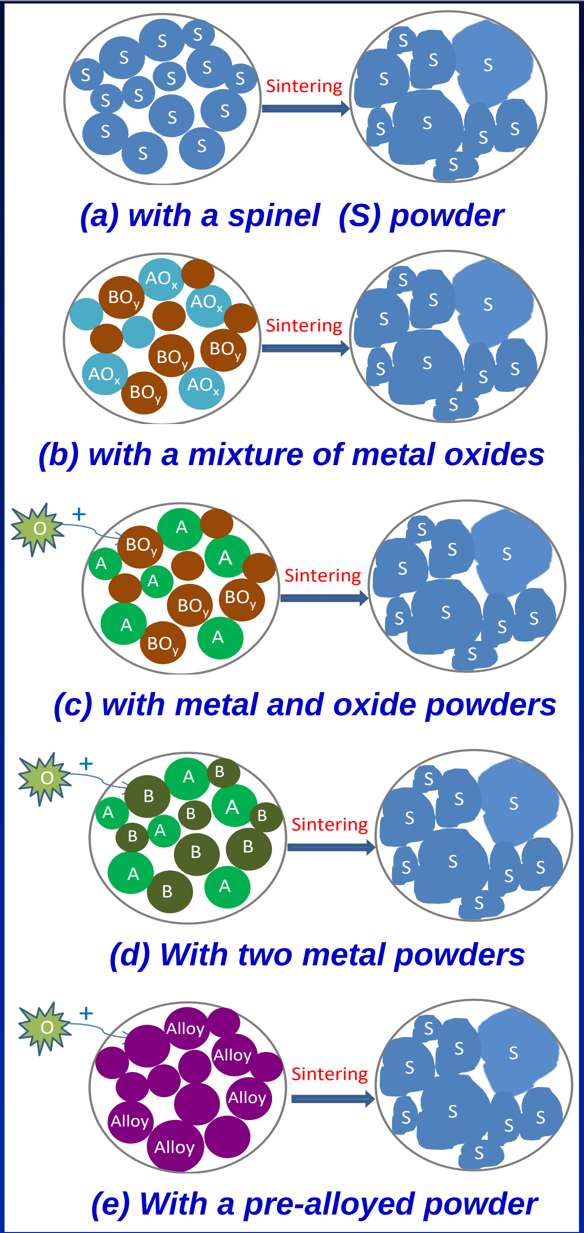


*(a) with a spinel (S) powder*

*(b) with a mixture of metal oxides*

*(c) with metal and oxide powders*

*(d) With two metal powders*

*(e) With a pre-alloyed powder*

# Project Objectives

- **Optimization of the multi-component alloy precursor composition as contact and coating materials.** The alloy compositions will be optimized via composition screening in the $(Ni,Fe,Co,X)_3O_4$ and $(Mn,Co,X)_3O_4$ systems, alloy design using physical metallurgy principles, and cost considerations. The desired alloy powders will be manufactured.
- **Demonstration/validation of the contact layer and interconnect coating performance in relevant SOFC stack environments.** Both ASR behavior and in-stack performance of the contact layer and interconnect coating in relevant stack operating environments will be evaluated.
- **Further cost reduction and commercialization assessment.** Approaches to further reducing the stack cost will be explored, such as co-sintering of the interconnect coating and contact layer during initial stack firing. Cost analysis and scale-up assessment will be conducted for potential commercialization.

# Composition Variation in $(Mn,Co)_3O_4$ Spinel

- Some controversies exist for the $Mn_2O_3$-$Co_3O_4$ system.
- Two most important compositions in the $(Mn,Co)_3O_4$ spinel system are:
  - ✓ $MnCo_2O_4$: CS at both 800 and 20°C;
  - ✓ $Mn_{1.5}Co_{1.5}O_4$: CS at 800°C and TS + CS at 20°C.
- Our previous study focused on the effect of spinel composition (x = 1 to 1.5) in $Mn_xCo_{3-x}O_4$ on its electrical conductivity and CTE.
- Several promising spinel compositions were identified accordingly.

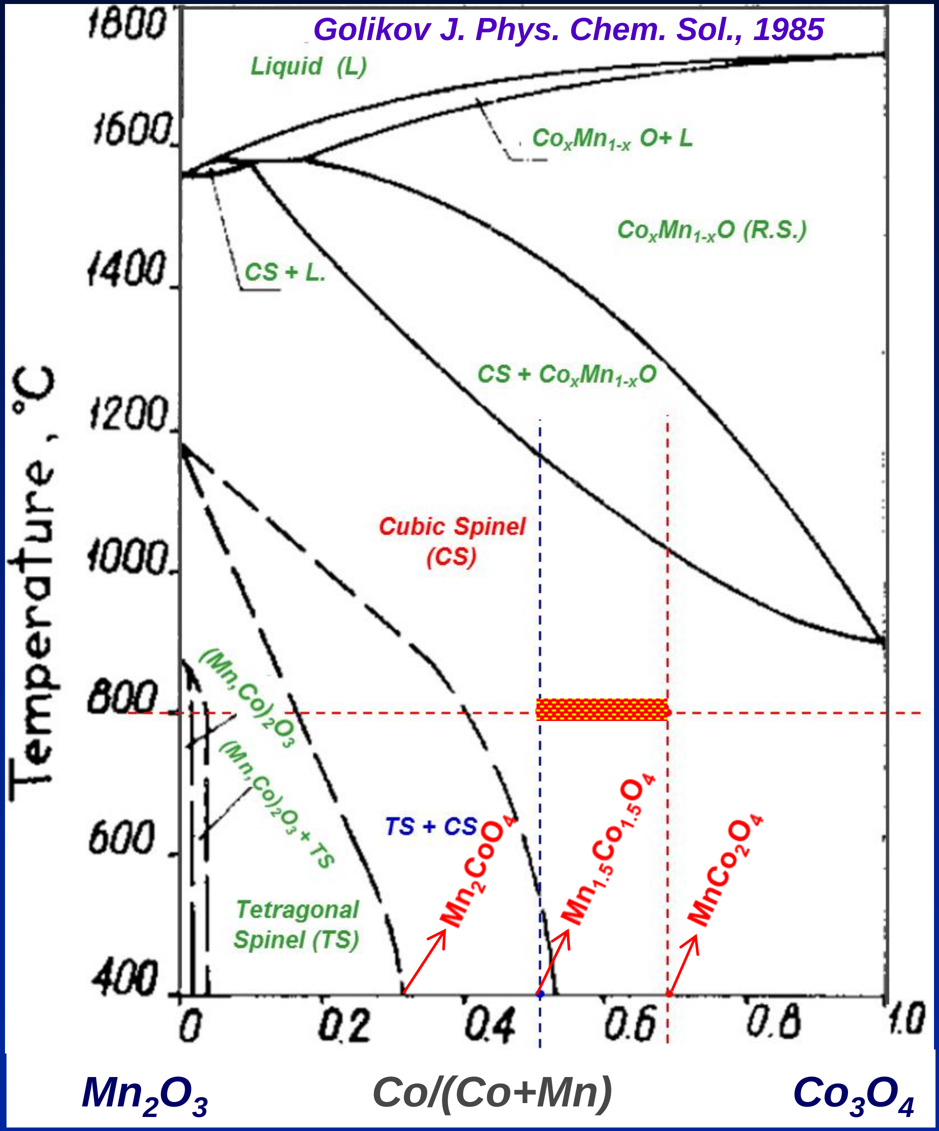


Phase Diagram of the Co-Mn-O System in Air

# Spinel Compositional Optimization in $(Mn,Co)_3O_4$: Reaction Layer (RL) Formation with $Cr_2O_3$

- **Polished pellets of $Mn_xCo_{3-x}O_4$ (x = 1.0, 1.2, 1.35, 1.5) and $Cr_2O_3$ were placed in contact with one another (with Pt nano-particles as markers of the original interface under a compressive load at 900°C for 20-700 h.**
- **The diffusion couples were then cross-sectioned for microstructural observation and the reaction layer composition/ thickness were determined.**

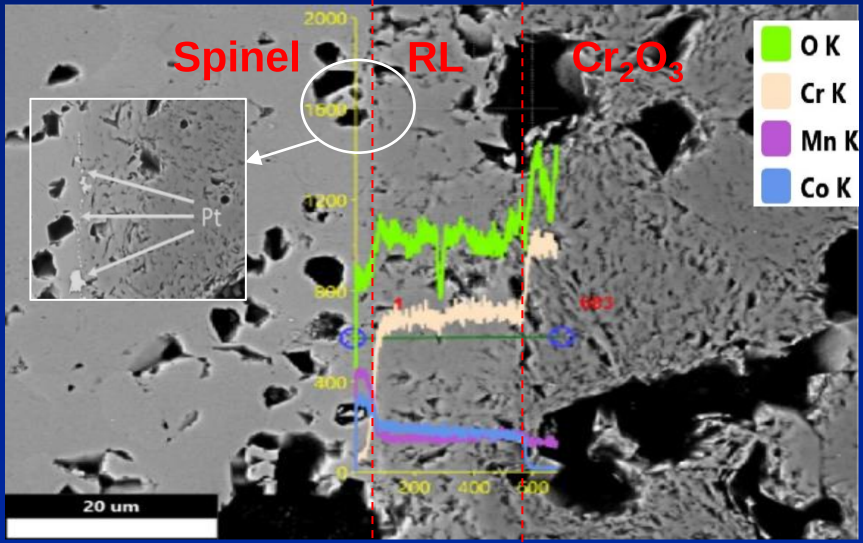


**$Mn_{1.35}Co_{1.65}O_4/Cr_2O_3$ Diffusion Couple Annealed for 300 h at 900°C**

**RL Compositions for $Mn_xCo_{3-x}O_4/Cr_2O_3$ Couples**

| Diffusion Couple | RL Composition |
|---|---|
| $MnCo_2O_4/Cr_2O_3$ | $Mn_{0.1}CoCr_{1.9}O_4$ |
| $Mn_{1.2}Co_{1.8}O_4/Cr_2O_3$ | $Mn_{0.15}Co_{0.95}Cr_{1.9}O_4$ |
| $Mn_{1.35}Co_{1.65}O_4/Cr_2O_3$ | $Mn_{0.5}CoCr_{1.5}O_4$ |
| $Mn_{1.5}Co_{1.5}O_4/Cr_2O_3$ | $Mn_{0.25}Co_{0.85}Cr_{1.9}O_4$ |

# Electrical Conductivity and CTE of the RL Compositions

- **The spinel RL exhibited overall lower electrical conductivity and CTE than the corresponding MCO spinels.**
- **$Mn_{0.5}CoCr_{1.5}O_4$ (formed in the $Mn_{1.35}Co_{1.65}O_4/Cr_2O_3$ couple) had a highest electrical conductivity and CTE among the RL compositions evaluated.**

**Electrical Conductivity and CTE of Different RL Compositions**

| Composition | σ at 800°C ($S\text{-}cm^{-1}$) | Average CTE ($\times10^{-6}\ K^{-1}$) |
|---|---|---|
| $Mn_{0.1}CoCr_{1.9}O_4$ | 0.30 | 7.46 |
| $Mn_{0.25}Co_{0.85}Cr_{1.9}O_4$ | 0.13 | 7.44 |
| $Mn_{0.5}CoCr_{1.5}O_4$ | 3.35 | 8.48 |

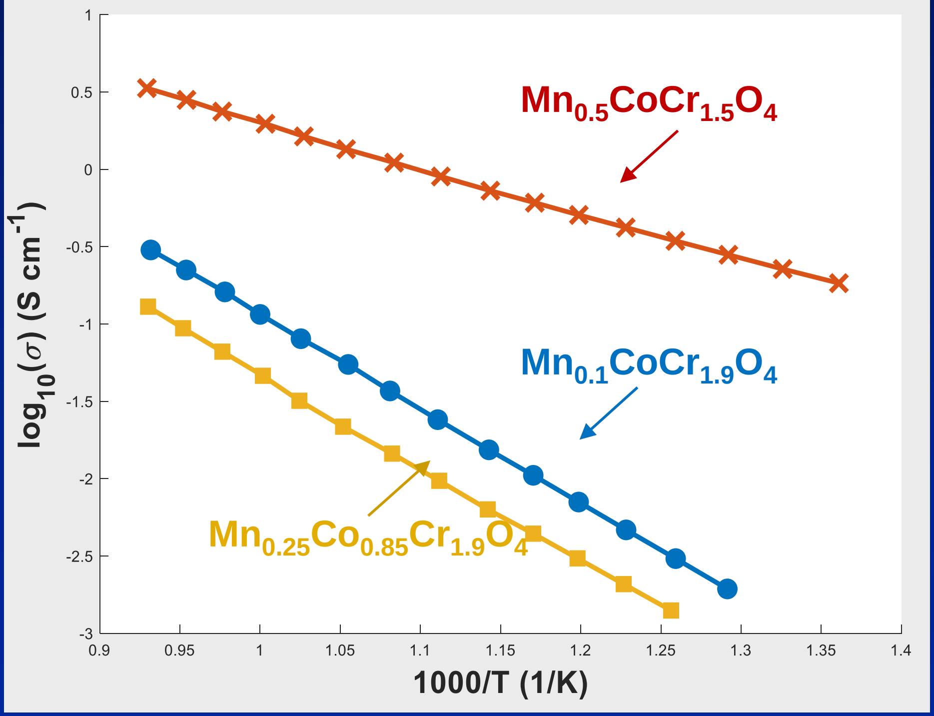


**Electrical Conductivity vs. 1/T of Different Reaction Layer Compositions**

# Growth Kinetics of Reaction Layer

- The RL growth rate increased with the Mn content in $Mn_xCo_{3-x}O_4$;
- The RL ASRs was projected based on both the layer growth kinetics and its electrical conductivity.
- Based on the projected RL ASR contribution, the $Mn_xCo_{3-x}O_4$ spinel with x ≤ 1.35 are most suitable for long-term operation.

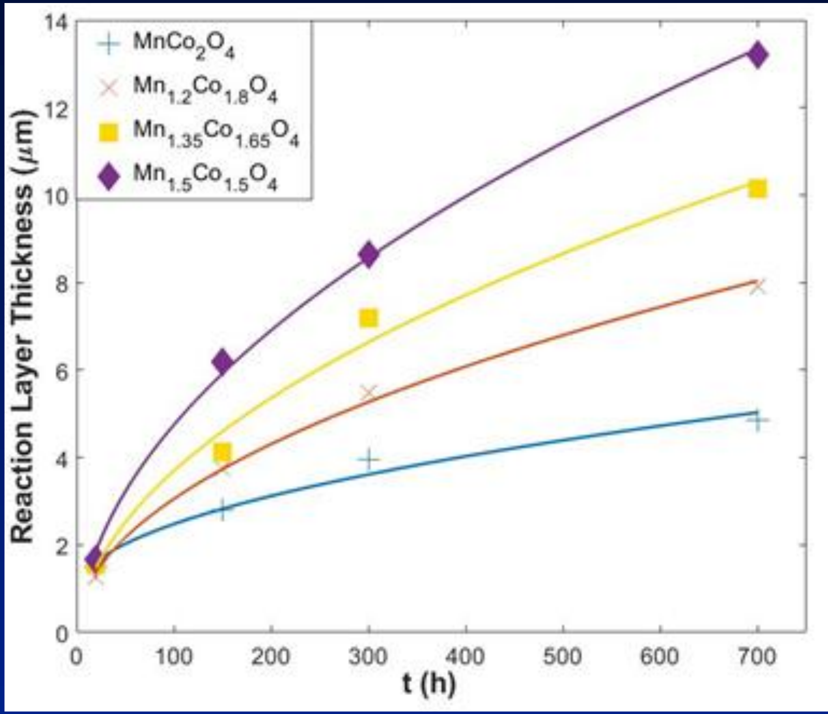


Thickness of the reaction layer vs. t

Projected ASR Values for Different Reaction

| Diffusion Couple | RL Composition | Projected RL ASR (mΩ·cm²) | | | |
|---|---|---|---|---|---|
| | | 5000 h | 10,000 h | 2,0000 h | 4,0000 h |
| $MnCo_2O_4/Cr_2O_3$ | $Mn_{0.1}CoCr_{1.9}O_4$ | 1.55 | 2.20 | 3.11 | 4.40 |
| $Mn_{1.35}Co_{1.65}O_4/Cr_2O_3$ | $Mn_{0.5}CoCr_{1.5}O_4$ | 0.44 | 0.60 | 0.88 | 1.24 |
| $Mn_{1.5}Co_{1.5}O_4/Cr_2O_3$ | $Mn_{0.25}Co_{0.85}Cr_{1.9}O_4$ | 8.99 | 12.71 | 17.97 | 25.42 |

# Gas Atomization of Co-Mn Based Alloys

- **Based on the properties of MCO, a number of Mn-Co based precursor alloy compositions were selected for gas atomization.**
- **The atomized powder precursor layers were successfully converted to a single-phase spinel structure after 900°C for 2 h in air.**

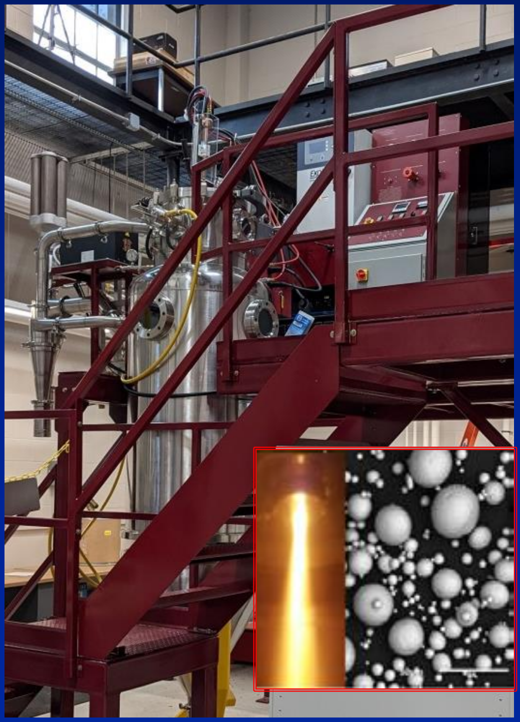

Gas Atomizer at TTU

**Chemical Compositions of Some Co-Mn Alloy Powders (wt.%) & Corresponding Spinel Compositions**

| Alloy | Co | Mn | Fe | Ce | Spinel Composition |
|---|---|---|---|---|---|
| Alloy 1 | 68.21 | 31.79 | — | — | $MnCo_2O_4$ |
| Alloy 2 | 64.72 | 31.80 | 3.23 | — | $MnCo_{1.9}Fe_{0.1}O_4$ |
| Alloy 3 | 64.72 | 31.77 | 3.23 | 0.41 | $MnCo_{1.895}Fe_{0.1}Ce_{0.005}O_4$ |

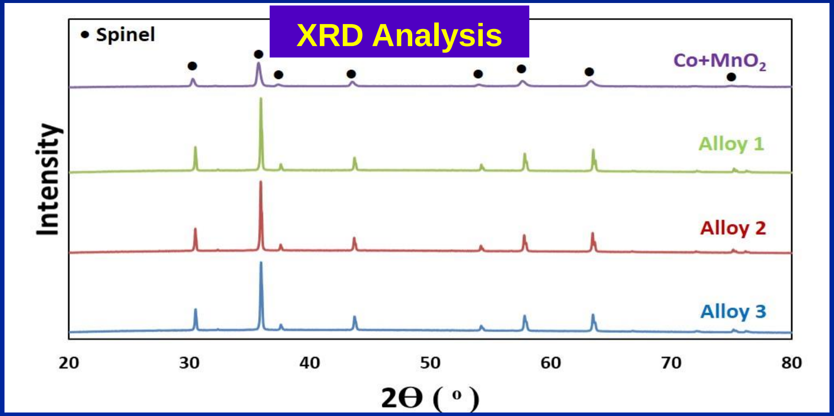


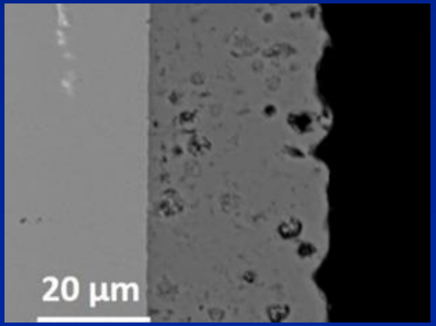


Cross-sectional View of Converted Alloy-1 Layer

# Cell Area-Specific Resistance (ASR) with Different Contact Layers

- A number of test cells were constructed, with the contact precursor layer sandwiched between bare Crofer 22 APU and the LSM cathode.
- The cell ASRs with all the alloy-derived contacts were significantly lower than that with the mixed Co+$MnO_2$ derived contact.
- The cell with the Ce-doped alloy (Alloy-3) contact had the best overall ASR performance.

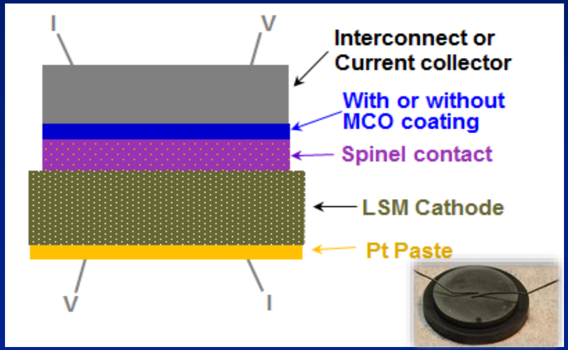


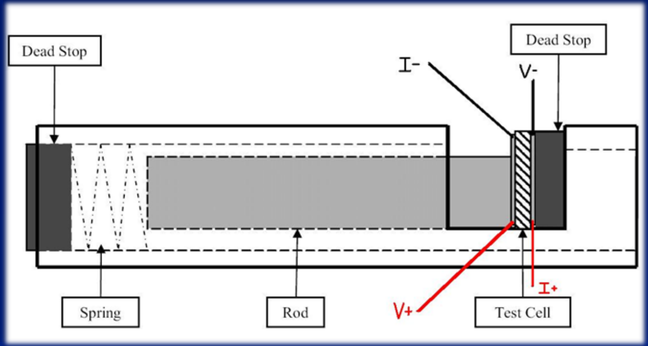


Schematic of ASR Test Cell

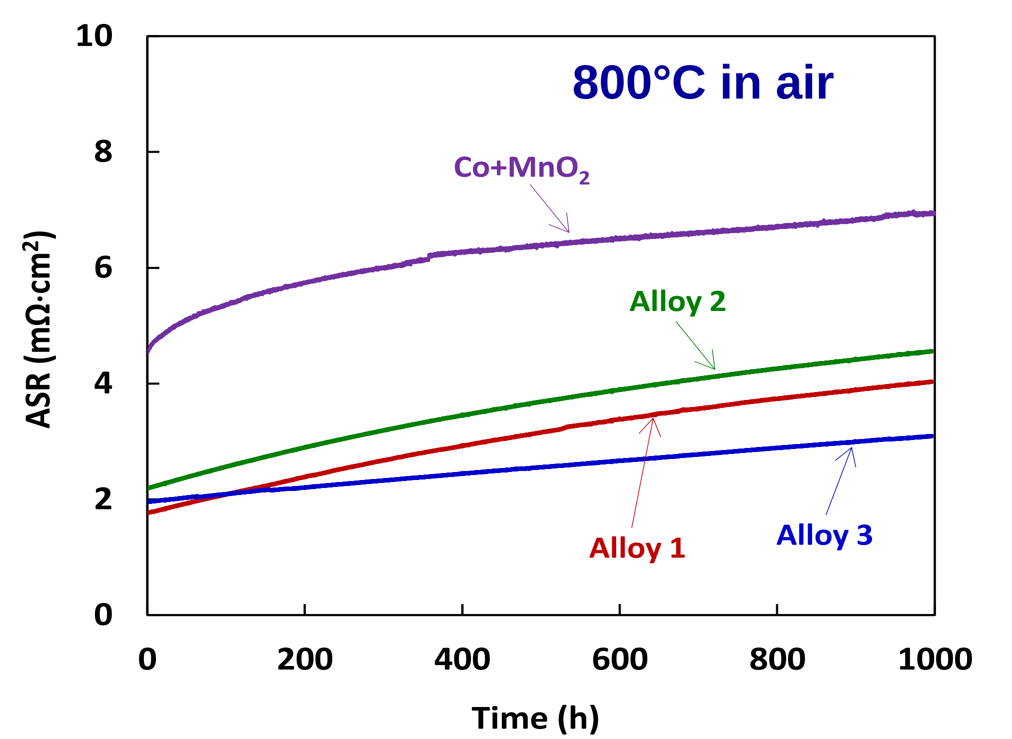


Cell ASR vs. Time of Test Cells

# Cell Area-Specific Resistance (ASR) with Different Contact Layers

- The cell ASR with Co+$MnO_2$ derived contact had the highest initial and final ASR ($R_i$ and $R_f$) as well as the highest initial and final ASR degradation rate ($DR_i$ and $DR_f$), likely due to the more porous nature of the contact layer.
- The cell ASR with Alloy-3 derived contact had the lowest $R_f$, $DR_i$ & $DR_f$, likely as a result of the Ce dopant modifying the $Cr_2O_3$ scale growth.

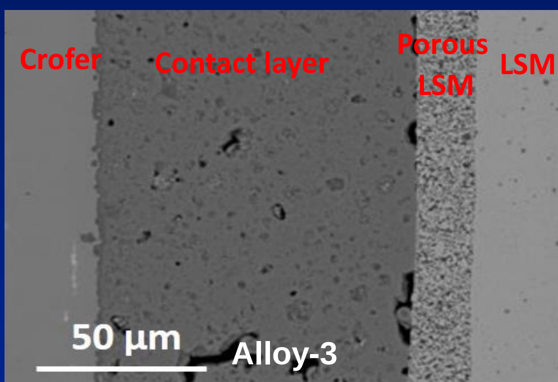


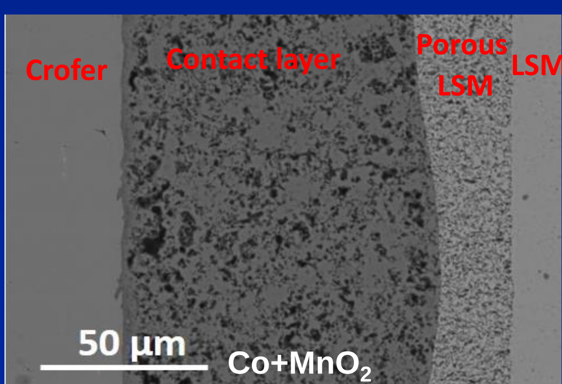


**Cell ASR at 800°C during Isothermal Exposure**

| | Alloy 1 | Alloy 2 | Alloy 3 | Co+$MnO_2$ |
|---|---|---|---|---|
| $R_i$ ($m\Omega \cdot cm^2$) | 1.8 | 2.2 | 2.0 | 4.6 |
| $R_f$ ($m\Omega \cdot cm^2$) | 4.0 | 4.6 | 3.1 | 7.0 |
| $DR_i$ ($\mu\Omega \cdot cm^2/h$) | 3.3 | 3.5 | 1.5 | 11.1 |
| $DR_f$ ($\mu\Omega \cdot cm^2/h$) | 1.4 | 1.3 | 1.0 | 1.4 |

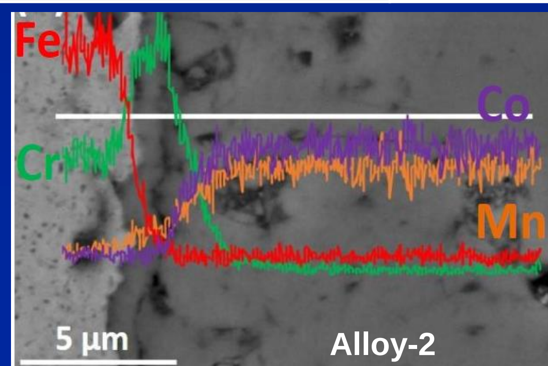


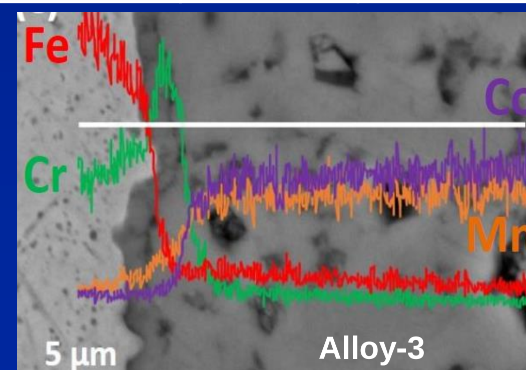

# ASR under Severe Cycling Condition

– The cells were cyclically exposed (one cycle consisted of holding at 800°C for 10 h, furnace cooled, and reheated to 800°C). In addition to the best MCO contact, two commercial contact materials were included in evaluation for comparison, i.e., $La(Mn_{0.45}Co_{0.35}Cu_{0.2})O_3$ (LCC10) & LSM.

– The cell with the EARS-processed MCO contact exhibited the lowest and most stable ASR over 500 cycles.

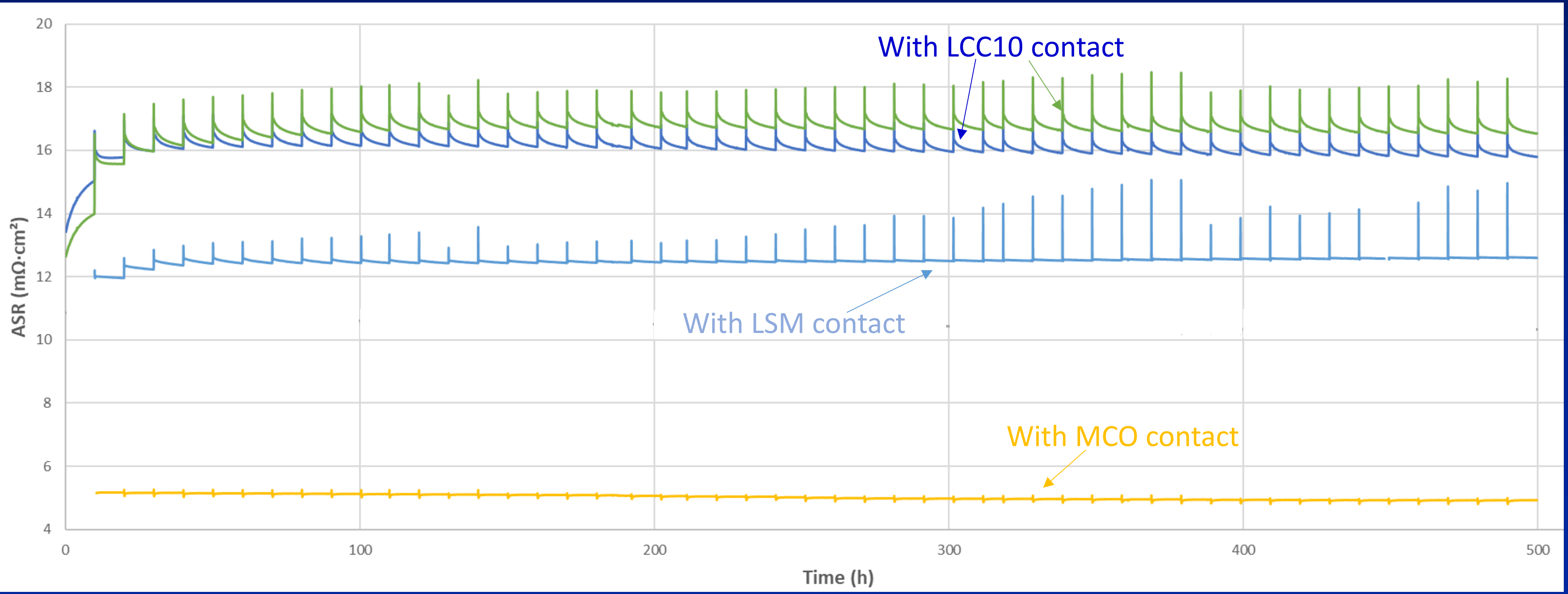


ASR vs. Cumulative Time during Cyclic Exposure for ZMG/Contact/LSM Cells

# EARS Processing of Dense MCO Coatings

- By controlling the composition/shape/size/size distribution/initial packing density of the metallic precursor powders, a uniform & dense spinel layer was achieved after thermal conversion at 900°C for 2 h in air on the full-size plate.
- The EARS-derived coating does not require a reduction treatment or a sintering temperature > 900°C.

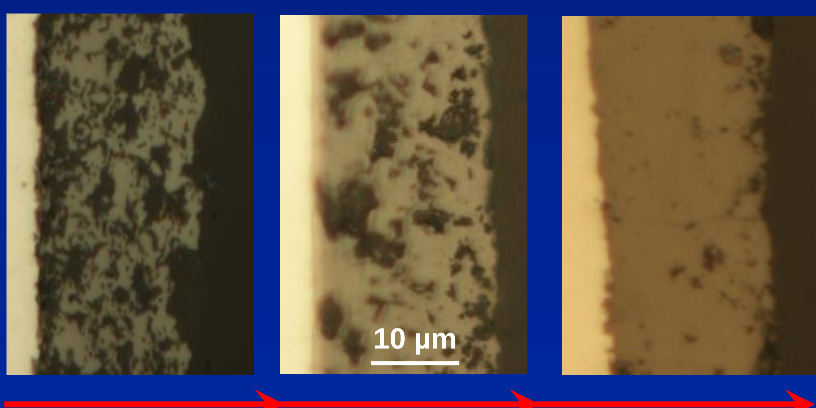


Improvement in Quality of TTU's Reactively Sintered MCO Coatings

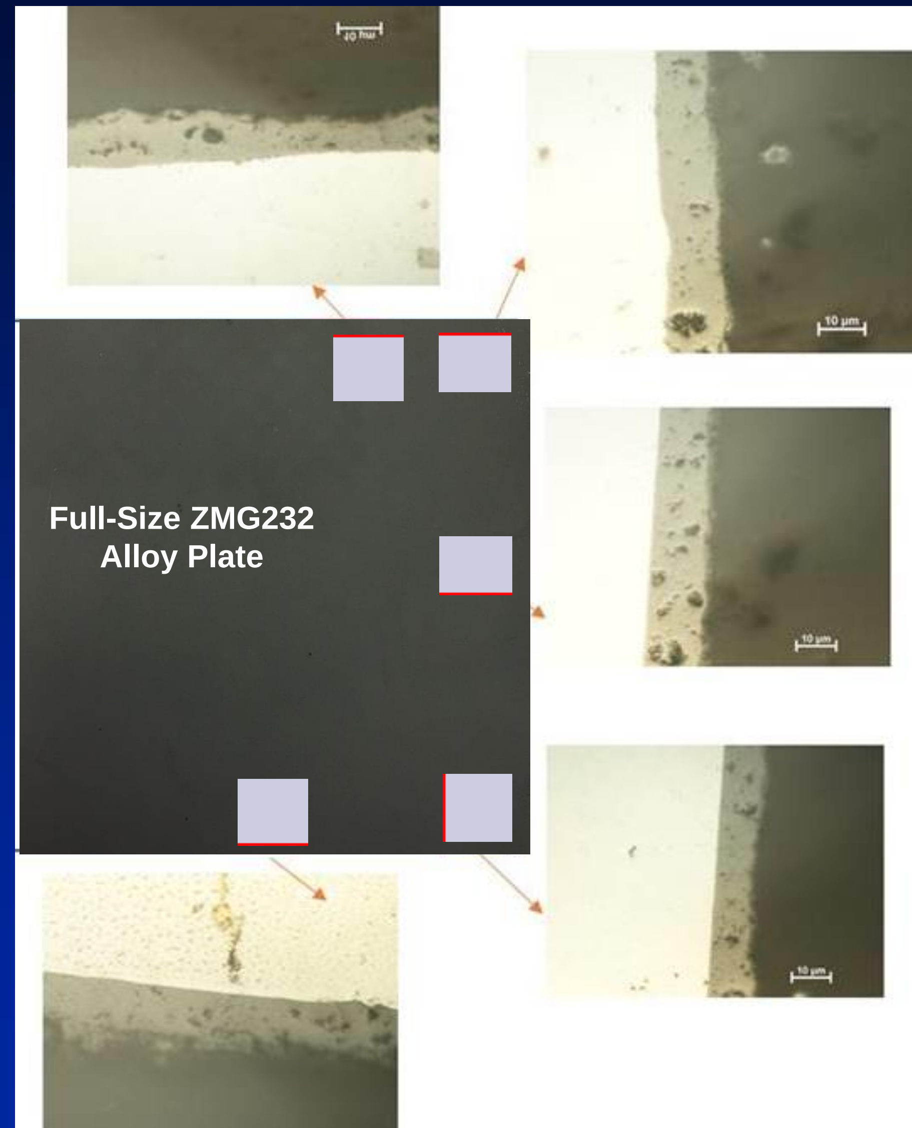


MCO Coating at Different Plate Locations

# Co-sintering of Coating/Contact Dual-Layer Structure: Proposed Approach

- To improve the contact quality and reduce the coating/contact processing cost, co-sintering of the coating and the contact layer during initial stack firing/operation is explored, utilizing two different metallic precursors:
  - Two spinel-forming precursors (Type #1 – for the contact layer and Type #2 – for the dense MCO coating) were employed;
  - Reactive co-sintering in air at 900°C was utilized for simultaneous formation of the dual-layer structure.

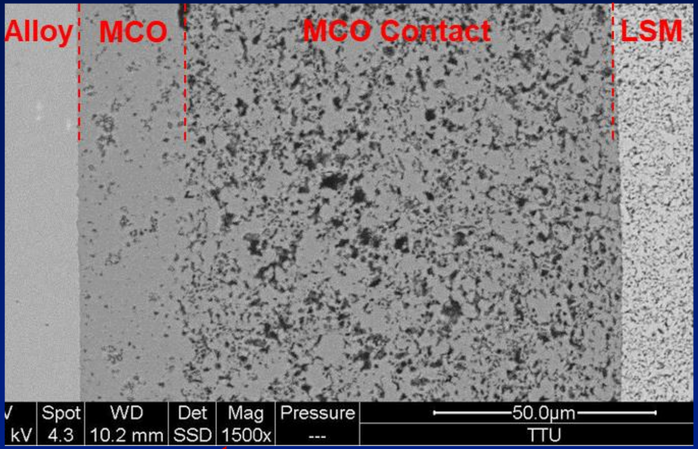


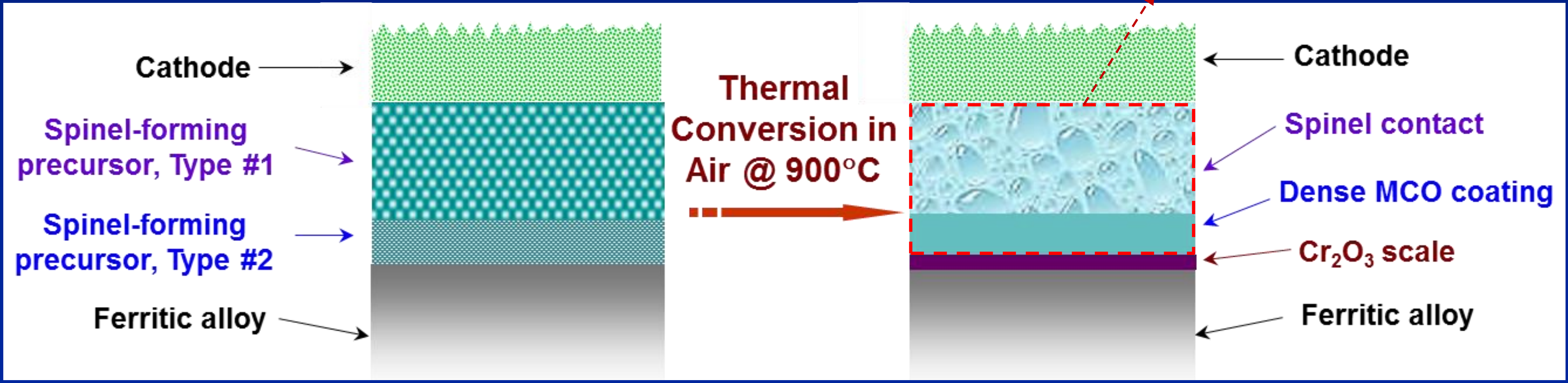


Schematic of Co-sintering of Spinel-Based Coating/Contact Dual-Layer Structure

# Low, Stable ASR of Full-Size ZMG230/Coating/Contact/LSM Assembly with Co-sintered Coating/Contact Layer

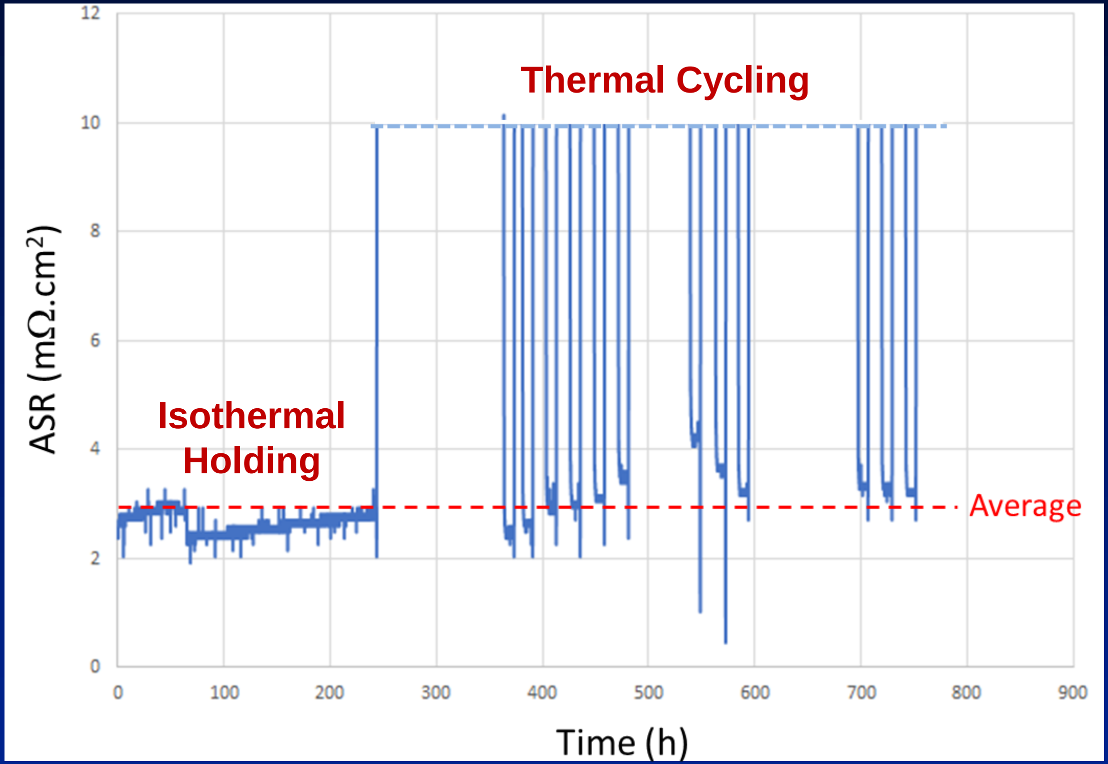


ASR during Isothermal and Cyclic Exposures at 800°C in Air for Full-Size ZMG/coating/ Contact/LSM Assembly Co-sintered at 900°C for 2 h.

- The warping problem of the 3-mm ZMG alloy plates during grinding was addressed by a stress-relief anneal treatment.
- Co-sintering of the double-layer structure between the full-size ZMG & LSM plates led to formation of the desired microstructures & low ASR.
- The negligible effect of thermal cycling on the ASR behavior is a result of nearly perfect match in CTE between these components.

# Concluding Remarks

- Several spinel compositions in the $(Mn,Co)_3O_4$ system have been identified for SOFC coating/contact applications, based on considerations of phase constitution, electrical conductivity, CTE, reaction layer formation with chromia, etc.
- A number of Mn-Co based precursor alloy powders have been prepared via gas atomization and good ASR performance of the EARS-processed spinel contact layer has been demonstrated.
- By controlling the metallic precursor powder characteristics, a dense MCO coating has been synthesized on full-size alloy plate.
- Co-sintered dual-layer structure with a dense spinel layer as coating and a porous layer as contact has shown exceptional electrical performance during isothermal and cyclic exposures.
- In-stack testing to verify the performance of co-sintered coating/ contact layers will be conducted by our industrial partner.
- Cost analysis & commercialization feasibility assessment has been initiated.

# Acknowledgments


- U. S. Department of Energy - National Energy Technology Laboratory, Solid Oxide Fuel Cell Prototype System Testing and Core Technology Development Program, Award No. DE-FE0031187; Project Manager: Dr. Patcharin Burke

- Allen Yu, Joseph Simpson, David Chesson, and Brian Bates, TTU

- Dr. Hossein Ghezel-Ayagh, FuelCell Energy, Inc.

- Dr. John Pietras and his team at Saint Gobain